ACS APPLIED MATERIALS & INTERFACES

Research Article

www.acsami.org

Plasma Polymer-Functionalized Silica Particles for Heavy Metals Removal

Behnam Akhavan, Karyn Jarvis, and Peter Majewski*

School of Engineering, Mawson Institute, University of South Australia, Mawson Lakes, SA 5095, Australia

ABSTRACT: Highly negatively charged particles were fabricated via an innovative plasma-assisted approach for the removal of heavy metal ions. Thiophene plasma polymerization was used to deposit sulfur-rich films onto silica particles followed by the introduction of oxidized sulfur functionalities, such as sulfonate and sulfonic acid, via water−plasma treatments. Surface chemistry analyses were conducted by X-ray photoelectron spectroscopy and time-of-flight secondary ion mass spectroscopy. Electrokinetic measurements quantified the zeta potentials and isoelectric points (IEPs) of modified particles and indicated significant decreases of zeta potentials and IEPs upon plasma modification of particles. Plasma polymerized thiophene-coated particles treated with water plasma for 10 min exhibited an IEP of less than 3.5. The effectiveness of developed surfaces in the adsorption of heavy metal ions was demonstrated through copper (Cu) and zinc (Zn) removal experiments. The removal of metal ions was examined through changing initial pH of solution, removal time, and mass of particles. Increasing the water plasma treatment time to 20 min significantly increased the metal removal efficiency (MRE) of modified particles, whereas further increasing the plasma treatment time reduced the MRE due to the influence of an ablation mechanism. The developed particulate surfaces were capable of removing more than 96.7% of both Cu and Zn ions in 1 h. The combination of plasma polymerization and oxidative plasma treatment is an effective method for the fabrication of new adsorbents for the removal of heavy metals.

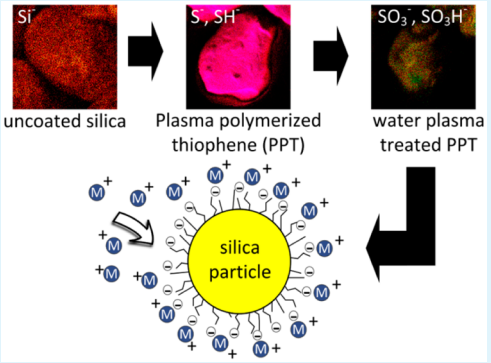

KEYWORDS: *plasma polymerization, plasma treatment, thiophene, water treatment, adsorption*

1. INTRODUCTION

The inadequate access to clean water is a serious worldwide problem that is expected to worsen in the near future.[1] Heavy metals are notorious for their detrimental effects on living organisms and are therefore considered as one of the most critical contaminants in water.[2] Copper and zinc, for example, are known as carcinogenic and mutagenic substances where their high intakes can cause liver, kidney, and pancreas damage.[3,4] Unlike organic pollutants, heavy metals do not break down into less harmful species over time.[4] Industrial activities including mining, metallurgy, painting, fertilizer, and battery manufacturing are the major sources of heavy metal releases into water.[3,5] The increasing rate of heavy metal production together with associated discharges into the environment further highlights the importance of heavy metals removal from water.[6]

The removal of heavy metals can be carried out via a number of remediation methods including chemical precipitation−coagulation,[7] membrane separation,[8] electrodialysis,[9] and adsorption.[10] Adsorption has gained particular interest in the past few years as an efficient, versatile, and low-cost choice.[2] This method is not only suitable for centralized water treatment plants but also for decentralized water treatment scenarios in remote areas and disaster zones.[11] Natural materials such as zeolites,[12] bentonite,[13] sugar beet pulp,[14] and clay[15] have been extensively studied in the literature for the removal of heavy metal ions. Although these low-cost adsorbents are readily available, they often exhibit slow kinetics and low removal efficiencies.[3,12] Such drawbacks have led to ongoing research for the fabrication of more efficient synthetic heavy metal adsorbents. The efficiency of synthetic adsorbents depends on the functionalities introduced onto the surface, which can either chemically or electrostatically adsorb the positively charged heavy metal ions.[2,16]

Particles functionalized with amine,[17] thiol,[18] and $-SO_x(H)$ groups such as sulfonic acid (SO_3H)[19] and sulfonate (SO_3)[20] have previously been applied for the effective removal of a number of divalent heavy metal ions such as Pb^{2+}, Cd^{2+}, Cu^{2+}, Co^{2+}, and Zn^{2+}. $-SO_x(H)$-functionalized particles are highly negatively charged in aqueous solutions over a wide pH range. The high negative surface charge of such modified particles makes them ideal electrostatic adsorbents for water purification.[16,19] The negative charge of $-SO_x(H)$-functionalized particles at low pH values is of particular interest for the removal of precious or hazardous metals from mining waste waters, which are often at low pH conditions.[21] Such functionalities are conventionally immobilized onto the surface of particles through wet-chemistry methods that are complex,

Received: December 8, 2014
Accepted: January 20, 2015
Published: January 20, 2015

DOI: 10.1021/am508637k
ACS Appl. Mater. Interfaces 2015, 7, 4265−4274

time-consuming, and dependent on substrate chemistry. Such technical hindrances, accompanied by a high rate of waste production, hamper the wide application of synthetic adsorbents. These issues can be addressed by developing an easy, rapid, and substrate-independent approach for the fabrication of heavy metals adsorbents, while minimizing the impact on the environment by keeping waste production low.

Plasma polymerization is a green approach that can be utilized as a novel alternative to traditional wet-chemistry methods for the fabrication of heavy metal adsorbents. Virtually all solid materials can be modified via this method, while minimal or no surface preparation is required. No solvent is involved in the process, and thus almost no waste is produced. In this technique, a precursor liquid monomer is initially converted to vapor, while being subsequently excited into the plasma under the influence of an electric field.[22] Plasma, also referred to as the fourth state of matter, is partially ionized gas consisting of neutral atoms and molecules, electrons, and charged particles.[23] The fragmented monomer species recombine onto any surface exposed to plasma and thus form a nanometers thin layer of plasma polymer film. Plasma polymer films are highly cross-linked and adherent to various substrates. Owing to these advantages, plasma polymerization technology can be applied for surface functionalization of particles regardless of their surface chemistry, size, and shape. Plasma surface modification of particles is more challenging than that of planar surfaces due to the large surface area in contact with plasma. To obtain a homogeneous distribution of functionalities onto particles, specified reactor designs such as rotating,[24] fluidized bed,[25] particle injection,[26] and magnetic stirrer[27] have been previously utilized. Our previous research has shown successful fabrication of hydrocarbon[28,29] and amine[11,30] functionalized silica particles via plasma polymerization technology for the removal of hydrophobic and negatively charged contaminants, respectively.

Unlike hydrocarbon and amine functionalities, the formation of $-SO_x(H)$ moieties onto a surface is unfortunately not feasible via a direct plasma polymerization process, as low volatile $-SO_x(H)$-containing monomers do not evaporate into the plasma chamber at ambient temperature.[31] A limited number of studies have been previously undertaken to generate $-SO_x(H)$ moieties onto surfaces through a plasma-assisted process without any wet-chemistry step being involved.[31−33] Sulfur dioxide (SO_2) has been utilized in these processes either for copolymerization or post-treatment of plasma polymers. These methods are, however, still environmentally questionable due to the toxicity of SO_2 gas. We recently reported a new method to generate such functionalities onto planar surfaces via a combination of plasma polymerization and oxidative plasma treatment.[34]

In this investigation, we report the fabrication of highly negatively charged adsorbent materials via water plasma (WP) treatment of plasma polymerized thiophene (PPT) films deposited onto silica particles. Silica particles were applied as substrates as they are low-cost, commercially available, and mechanically stable. The WP treatment time was varied from 2 to 60 min to study its effect on surface chemistry, zeta potential, and heavy metal removal efficiency (MRE). The MRE of WP-treated plasma polymerized thiophene (WP-PPT) coated particles was evaluated through the adsorption of copper and zinc as model positively charged heavy metal ions. The initial pH of solution, removal time, and mass of particles were varied to maximize the removal of heavy metal ions. The surface engineering of silica particles through the deposition of PPT films followed by an oxidative WP treatment is an effective dry route to develop a new class of adsorbent materials for the removal of cationic contaminants.

2. EXPERIMENTAL SECTION

2.1. Materials. Crystalline silica particles with particle sizes in the range of 200−300 μm, thiophene (C_4H_4S) monomer, copper nitrate trihydrate ($Cu(NO_3)_2{\cdot}3H_2O$), and zinc nitrate hexahydrate ($Zn(NO_3)_2{\cdot}6H_2O$) were obtained from Sigma-Aldrich (Castle Hill, Australia) and used without any further treatment.

2.2. Plasma Polymerization. Plasma polymerization of thiophene onto silica particles and WP treatment of PPT-coated particles were conducted using a custom-built rotating plasma polymerization reactor, which has been previously detailed.[29] The reactor was operated by a 13.56 MHz radio frequency (RF) generator and matching network (Coaxial Power Systems, Ltd.). The rotating barrel made of Pyrex tube (L = 0.5 m, D = 0.16 m, V = 10.05 L) was equipped with a mixing paddle to ensure the homogeneous exposure of particles to plasma during both plasma polymerization and treatment processes. Liquid monomer thiophene and Milli-Q water were degassed via at least three freeze−thaw cycles, while the base pressure of less than 7×10^{-3} mbar was achieved in the chamber. The flow rates of thiophene and water vapor were adjusted using a needle valve. For each batch of samples, thiophene was initially plasma polymerized onto 50 g of silica particles at an RF input power of 8 W and monomer flow rate of 6 standard cubic centimeters per minute (sccm) for a polymerization time of 30 min to obtain sufficiently thick PPT layers.[35] PPT-coated particles were subsequently treated with WP without being removed from the chamber. WP-treated samples were produced for varied plasma treatment times of 2 to 60 min, while the plasma input power of 5 W and water vapor flow rate of 2 sccm were kept constant. For both plasma polymerization and WP treatment processes, a rotating speed of 16 rpm was kept unchanged.

2.3. X-ray Photoelectron Spectroscopy. The surface chemistry of untreated and WP-treated PPT-coated silica particles was analyzed by X-ray photoelectron spectroscopy (XPS) using a SPECS SAGE instrument equipped with a hemispherical analyzer (Phoibos 150), an MCD-9 detector, and a Mg Kα source ($h\nu$ =1253.6 eV) operating at 200 W (10 kV, 20 mA). The takeoff angle was 90°, while the chamber pressure was at least 10×10^{-6} Pa. Samples were mounted onto 1 cm circular pieces of carbon tape, and the analysis area was set to 5 mm in diameter. Survey spectra were obtained from 0 to 1000 eV with a pass energy of 100 eV and energy steps of 0.5 eV, while high-resolution S 2p spectra (0.1 eV) were recorded at a pass energy of 20 eV. Calculations of survey atomic concentrations and curve fittings of S 2p high-resolution spectra were carried out by CasaXPS software. Charge correction was conducted in reference to the binding energy of aliphatic carbon (285.0 eV). A linear background, Gaussian (70%)−Lorentzian (30%) line shape, and equal full-width at half-maximum (fwhm) were applied. Systematic errors related to peak fittings, calculations of atomic concentrations, and experimental settings are assumed to be less than 10%.[31]

2.4. Time of Flight Secondary Ion Mass Spectroscopy. TOF-SIMS negative ion distribution maps were obtained using a PHI TRIFT V nanoTOF instrument (Physical Electronics Inc., Chanhassen, MN, USA). The instrument was equipped with a 30 eV $^{79}Au^+$ pulsed liquid metal primary ion gun (LMIG), while the base pressure of 5×10^{-6} Pa or lower was applied. "Unbunched" Au_1 instrumental configurations provided optimized spatial resolution for images. An electron flood gun and 10 eV Ar^+ ions provided dual charge neutralization. Negative SIMS counts were collected over scan areas of ~400 × 400 μm. Ion distribution images were processed using WincadenceN software provided by Physical Electronics Inc. (Chanhassen, MN, USA).

2.5. Environmental Scanning Electron Microscopy. Microscopic images of uncoated and untreated/treated PPT-coated silica particles were acquired using an environmental scanning electron microscopy (ESEM, FEI Quanta 450 FEG ESEM). The microscope

DOI: 10.1021/am508637k
ACS Appl. Mater. Interfaces 2015, 7, 4265−4274

was operated at 20 kV, while a pressure of 100 Pa and a typical working distance of 7 mm were applied. Images were obtained in both secondary and backscattered electron modes, using the large field gaseous secondary electron detector and the solid state backscattered electron detector. A mixture of these signals that best highlighted the sample contrast was used in the final images.

2.6. Electrokinetic Analysis. Zeta potential measurements of untreated and WP-treated PPT-coated particles were undertaken using an Anton Paar Electro Kinetic Analyzer in a pH range of 3−10. The pH of the electrolyte was adjusted using a remote titration device. Particles were packed into a cylindrical powder cell (1 cm in diameter and 1 cm long). The packed cell was then placed in the middle of a cylindrical unit with Ag/AgCl electrodes. The 1×10^{-3} M KCl solution was applied as electrolyte with an initial pH of ∼10, which was adjusted by appropriate volumes of 0.1 M KOH. Appropriate volumes of 0.1 M HCl were injected into the electrolyte solution by the remote titration unit to reduce the pH by ∼0.5 unit steps. As the electrolyte solution was pumped from left to right and right to left, zeta potential measurements were taken at each pH value. For every sample, three measurements were taken, providing six values for each data point. The averaged values were reported as the final zeta potential for a specific pH.

2.7. Heavy Metals Removal Tests. Copper and zinc batch removal tests were carried out at room temperature in glass beakers. Stock solutions of copper or zinc (100 mg/L) were prepared by dissolving their nitrate salts ($Cu(NO_3)_2{\cdot}3H_2O$ and $Zn(NO_3)_2{\cdot}6H_2O$) in Milli-Q water. Solutions of copper or zinc at a concentration of 15 mg/L were prepared by diluting appropriate volumes of stock solutions. A fixed solution volume of 10 mL was used for all removal tests. The influence of surface chemistry on the removal of metal ions at pH values of 3.5, 4.5, and 5.5 was studied by adding 2 g of particles, treated for different times, to the 15 mg/L solutions. The suspensions were stirred on a magnetic stirrer for 10 min. Particles were then separated by filtration with a 0.45 μm hydrophilic cellulose acetate filter. Removal time variable experiments were conducted by adding 2 g of WP-PPT-coated particles (WP treatment time = 10 min) to zinc or copper solutions with an optimum initial pH of 5.5, and stirring time was varied from 0.5 to 120 min. The influence of mass of particles on the removal of metal ions was evaluated by adding 0.25 to 5 g of WP-PPT-coated particles (WP treatment time = 10 min) to zinc or copper solutions, while optimum initial pH of 5.5 and removal time of 60 min were kept unchanged. The concentration of copper or zinc ions in filtrates was measured using an inductively coupled plasma-optical emission spectroscopy (ICP-OES) (PerkinElmer − Optima 5300 V) with a detection limit of 0.5 mg/L for copper or zinc. Continuous calibration verification (CCV) tests were conducted after each 10 measurements, which showed deviations of less than 10% from the standard solutions. The MRE was calculated by

$$\mathrm{MRE} = \frac{c_i - c_f}{c_i} \times 100$$

Where C_i is the initial concentration of copper or zinc, and C_f is the concentration of residual metal ions after a removal experiment. Adsorption tests were conducted in duplicate, and averaged values are reported.

3. RESULTS AND DISCUSSION

3.1. Surface Chemistry of WP-PPT Coated Particles. Plasma polymer-functionalized adsorbents for heavy metal removal were produced via a two-step process: deposition of PPT films on silica particles followed by an oxidative WP treatment. XPS analysis of uncoated silica particles showed atomic concentrations of 29.2%, 54.6%, and 16.2% for silicon, oxygen, and carbon, respectively. PPT coatings were deposited onto silica particles at an optimum power-to-flow rate ratio (W/F) of 0.08 kJ·cm^{-3} for 30 min,[35] while WP treatments were conducted at a W/F ratio of 0.15 kJ·cm^{-3}. Our recent study on planar surfaces showed that oxidative plasma treatment of PPT films at W/F ratios lower than 0.45 kJ·cm^{-3} produces maximum concentration of $-SO_x(H)$ functional groups on the surface.[34] The XPS elemental compositions of untreated and WP-treated PPT-coated particles as a function of plasma treatment time is depicted in Figure 1. XPS analysis of untreated PPT-coated

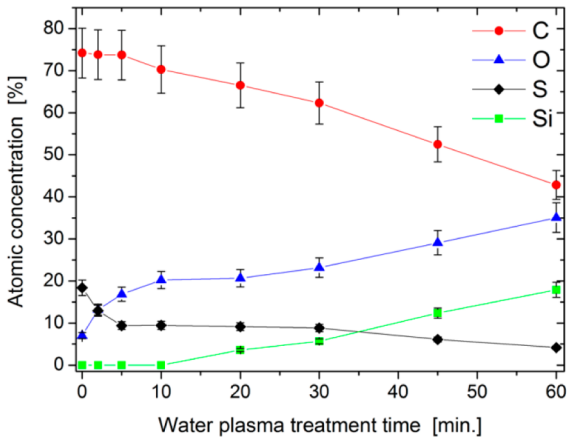

Figure 1. XPS survey elemental composition of untreated and WP-treated PPT-coated particles as a function of treatment time.

particles showed atomic concentrations of 75.2%, 18.0%, and 6.8% for carbon, sulfur, and oxygen, respectively, while no contribution from silicon was observed. The increases of sulfur and carbon atomic concentrations indicate the deposition of carbon- and sulfur-containing species onto the surface due to the fragmentation and subsequent reconstruction of thiophene rings.[36] Although the film thickness of PPT films deposited on silica particles cannot be directly measured via conventional methods such as profilometry and ellipsometry, it can be indirectly estimated through changes of silicon signals originating from the silica substrate. The sampling depth of XPS is 8−10 nm for a Mg Kα source and a takeoff angle of 90°.[11] The absence of silicon signals therefore indicates the deposition of a PPT layer with a thickness of at least 8 nm. Upon WP treatment of PPT-coated particles for up to 60 min, the atomic concentration of oxygen increases, while that of carbon and sulfur decrease. By increasing the treatment time over 10 min, silicon signals also start to significantly contribute in the overall spectra. The oxygen atomic concentration increases from 6.8% for untreated PPT-coated particles to 20.2% for PPT-coated particles treated for 10 min. As still no silicon is contributing in the surface chemistry of the sample treated for 10 min, it can be concluded that such an increase in oxygen atomic concentration is solely due to the incorporation of oxygen atoms into the structure of PPT film and not from the underlying silica substrates. The formation of sulfur−oxygen groups can be explained by an activation/oxidation mechanism.[37] According to this theory, reactive long-lived sulfur-centered radicals are initially generated onto the surface via hydrogen abstraction or polymer chain scission and are subsequently oxidized into stable groups via interactions with O and OH radicals. Generated long-lived radicals are also highly susceptible for post-treatment oxidation once exposed to atmospheric oxygen.[38]

The oxidative plasma treatment of polymers is, however, always accompanied by a degree of ablation process.[31] Water plasma may etch the PPT layer due either to physical interactions by high energy ions or to chemical reactions

DOI: 10.1021/am508637k
ACS Appl. Mater. Interfaces 2015, 7, 4265−4274

forming volatile species.[39] The influence of this concurrent process in the oxidation of PPT-coated particles is highlighted for samples treated for longer than 10 min. The contribution of silicon in the surface chemistry of these samples indicates the reduction of PPT film thickness to less than 8 nm, which therefore reveals the substrate silicon signals. The significant reduction of sulfur and carbon atomic concentrations can thus be attributed to both incorporation of oxygen atoms in the film structure and contribution of silica substrate to the overall spectra. While higher concentrations of sulfur-containing moieties need to be obtained on the surface for optimum removal efficiencies, further increasing the plasma treatment time over 60 min is not beneficial.

Sulfur high-resolution spectra of untreated and WP-treated PPT-coated particles were curve-fitted to study the formation of $-SO_x(H)$ moieties on the surface. Representative curve-fitted spectra of untreated PPT-coated particles and samples treated for 2, 10, and 60 min are shown in Figure 2. The S 2p

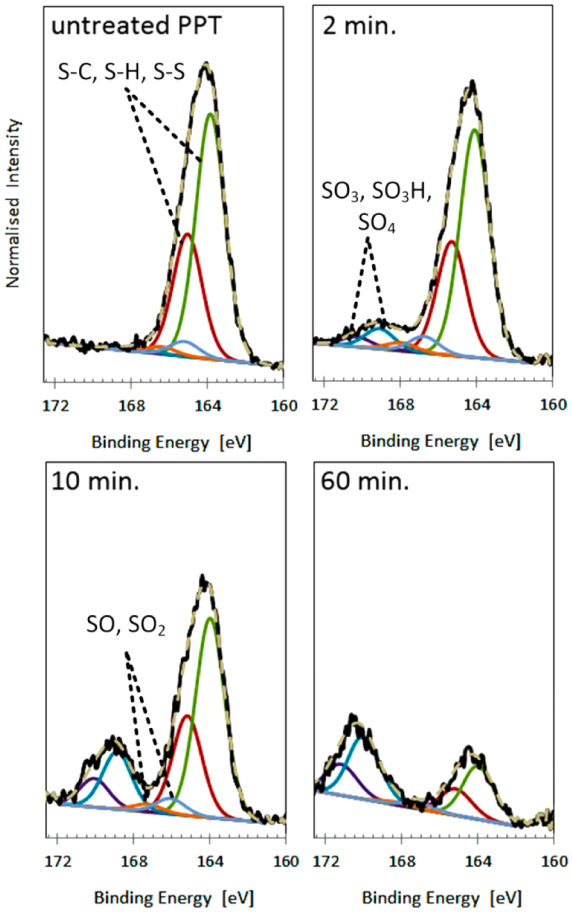

Figure 2. XPS S 2p curve-fitted spectra of untreated PPT-coated particles and PPT-coated particles treated with WP for 2, 10, and 60 min.

peak is doublet due to the spin−orbit coupling of S $2p_{1/2}$ and S $2p_{3/2}$ with an associated splitting binding energy (BE) of 1.2 eV.[40] The ratio of S $2p_{1/2}$ to S $2p_{3/2}$ was fixed to 1/2, as the photoionization cross-section of S $2p_{1/2}$ is half that of S $2p_{3/2}$.[31] According to the literature,[31,41] three doublet peaks were fitted in S 2p high-resolution spectra associated with (i) sulfur-containing compounds in neutral environments (S−H, S−C, and S−S) at BE = 163−165 eV, (ii) sulfur−oxygen compounds at low oxidation states (S−O and SO_2) at BE = 165−167 eV and (iii) sulfur−oxygen compounds at high oxidation states (SO_3H, SO_3, and SO_4) at BE = 167−169 eV, giving a total of six peaks. The individual identification of these compounds is not however possible via curve-fitting studies as the differences of associated binding energies are too low in comparison to the XPS resolution.[41] From Figure 2, it is apparent that upon WP treatment of PPT-coated particles, sulfur−oxygen groups emerge at BE > 166 eV. The concentration of these sulfur−oxygen compounds are quantified from peak-fitted spectra and plotted in Figure 3. More than 90% of sulfur compounds for

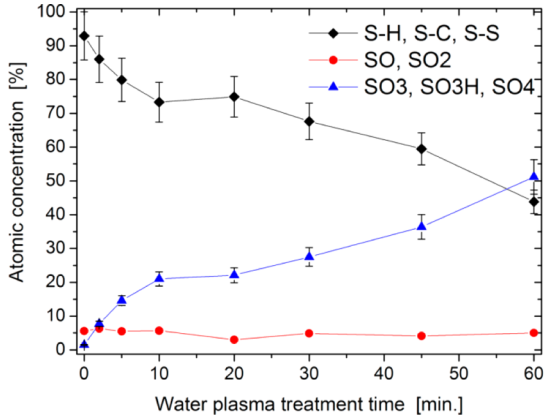

Figure 3. XPS atomic concentrations of curve-fitted S 2p components for untreated and WP-treated PPT-coated particles as a function of treatment time.

untreated PPT-coated particles are in the neutral environment, and only less than 10% of sulfur−oxygen groups contribute in the S 2p high-resolution spectra. By increasing the plasma treatment time, the concentration of oxidized sulfur moieties at high oxidation states increases, while that of sulfur compounds in the neutral environment significantly decreases. In contrast to highly oxidized sulfur groups (SO_3, SO_3H, SO_4), the concentration of sulfur−oxygen compounds at low oxidation states (SO and SO_2) remain relatively constant as the plasma treatment time increases. Such behavior may be attributed to the greater stability of highly oxidized sulfur compounds compared to partially oxidized SO and SO_2 groups.

The surface chemistry of modified silica particles was further studied via TOF-SIMS negative ion distribution maps displayed in Figure 4. As observed, plasma polymerization of thiophene onto silica particles results in a significant increase of S^- and SH^- species and elimination of Si^- counts. Such changes in negative ions counts were expected due to the polymerization of thiophene, which adds sulfur-containing species on the surface, while concealing silicon signals originating from the silica particles. For untreated PPT-coated particles, it is evident that sulfur species in a neutral environment (S^- and SH^-) are of significantly higher density in comparison to sulfur−oxygen species (SO_3^- and SO_3H^-). Upon WP treatment of PPT-coated particles, the density of S^- and SH^- counts, however, decrease, while that of oxidized sulfur species increase. The comparison of SO_3^- and SO_3H^- ion distribution maps of untreated PPT-coated particles to those treated for 10 min highlights the substantial increase of $-SO_x(H)$ functionalities. As previously discussed, such variations in surface chemistry denote the effectiveness of WP treatment for the development of sulfur-containing species through an activation/oxidation mechanism.

DOI: 10.1021/am508637k
ACS Appl. Mater. Interfaces 2015, 7, 4265−4274

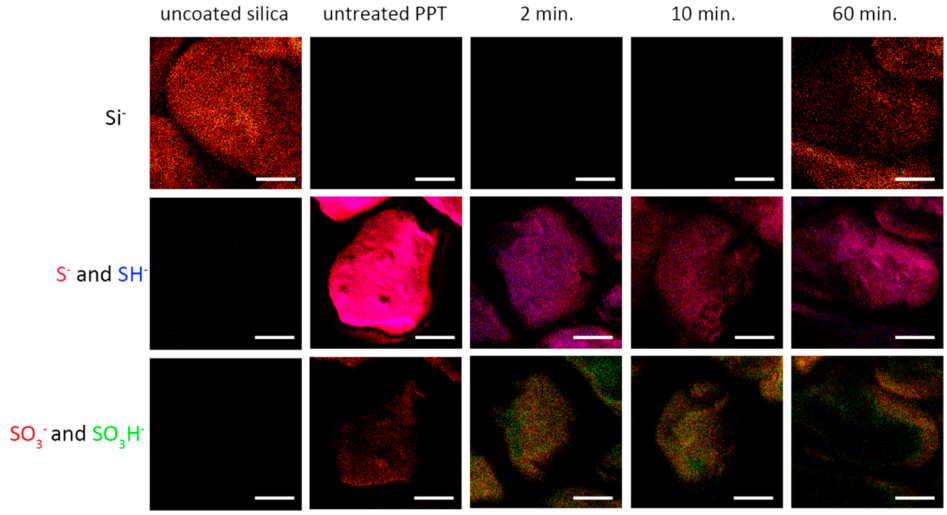

Figure 4. TOF-SIMS distribution maps of (Si^-), (S^-, SH^-), and (SO_3^-, SO_3H^-) for uncoated silica particles, untreated PPT-coated particles, and PPT-coated particles treated for different durations. (scale bar = 100 μm).

Water plasma treatment of PPT-coated particles for an extended duration of 60 min, however, exhibits a negative effect on the density of both S^-/SH^- and SO_3^-/SO_3H^- counts. It is observed that the decrease of sulfur-containing species is accompanied by noticeable increase in Si^- counts in the recorded data. According to the sensitivity depth of TOF-SIMS (1–2 nm),[42] the detection of Si^- counts implies a film thickness of less than 2 nm. Such a reduction in film thickness can be once again associated with the concurrent ablation mechanism as suggested by XPS data (Figure 1). The high spatial resolution of TOF-SIMS also provides the opportunity to disclose any possible inhomogeneity of the coating. As observed from Figure 4, TOF-SIMS images closely reveal the rough shape of silica particles for both untreated and treated PPT-coated particles, demonstrating the uniform distribution of functional groups. The deposition of homogeneous coatings on particles is of particular importance to obtain efficient adsorbents for heavy metal removal. These TOF-SIMS findings further support the XPS results and demonstrate the successful generation of $-SO_x(H)$ functionalities onto silica particles via a combination of thiophene plasma polymerization and WP treatment.

3.2. Morphology of WP-PPT-Coated Particles. ESEM micrographs of uncoated and untreated/treated PPT-coated silica particles are shown in Figure 5. Although homogeneous thin (a few nanometers thick) plasma polymer films were not expected to be visible on the particulate surfaces, ESEM images provided useful information regarding the preserved morphology of silica particles. From these images it is clear that after both plasma polymerization and plasma treatment processes, individual particles are still completely separated from each other and that no agglomeration has occurred. In surface engineering of particulate surfaces, the agglomeration of particles must be avoided as it reduces the effective surface area in practical applications such as water purification.[28,43] Agglomeration of particles during plasma polymerization/treatment would also result in the modification of only the outer layer of the agglomerates.[26,29] ESEM images, along with surface chemistry results, demonstrate that plasma polymerization/treatment using a rotating barrel plasma reactor is an effective approach for the deposition of $-SO_x(H)$-functionalized coatings onto particulate surfaces without altering the substrate morphology.

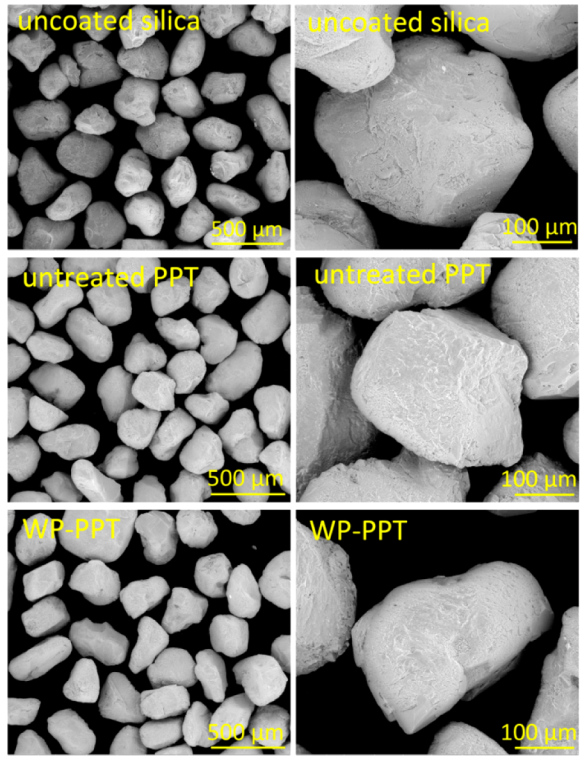

Figure 5. ESEM micrographs of uncoated silica particles and untreated and WP-treated PPT-coated particles (WP-PPT) (WP treatment time = 10 min).

3.3. Electrokinetic Properties of WP-PPT-Coated Particles. The surface charge of particles is of great importance for adsorption applications. For the removal of positively charged contaminants, such as heavy metal ions, it is ideally required to produce adsorbents with the lowest zeta potentials over the greatest pH range.[44] The influence of developed sulfur-containing functionalities on the isoelectric point (IEP) and zeta potential of particles was investigated via electrokinetic analysis. The zeta potential of a functionalized surface is highly pH-dependent as the dissociation of surface functionalities

DOI: 10.1021/am508637k
ACS Appl. Mater. Interfaces 2015, 7, 4265–4274

varies with pH.[45] The zeta potentials of particles are plotted as a function of pH and are shown in Figure 6. To conduct

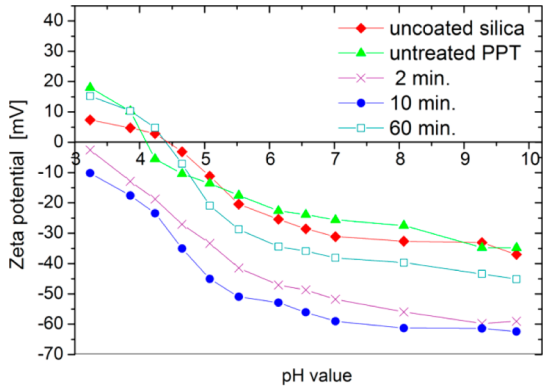

Figure 6. Zeta potential of uncoated silica particles, untreated PPT-coated particles, and PPT-coated particles treated with WP for different durations as a function of pH.

measurements at a constant ionic strength, the pH value was not reduced to lower than 3. High volumes of HCl are required to further decrease the pH, thus also significantly increasing the ionic strength. It is observed that the zeta potentials of all samples decrease as a function of pH due to the higher rate of deprotonation reactions at higher pH values.[11] Uncoated and PPT-coated silica particles show IEP values at pH values of ~5 and 4, respectively. The negative zeta potentials of uncoated and PPT-coated silica particles at pH > IEP result from the dissociation of silanol groups ($Si{-}OH \rightarrow Si{-}O^- + H^+$)[46] and deprotonation of neutral sulfur-containing groups such as thiol functionalities ($RSH \rightarrow RS^- + H^+$),[44] respectively. The positive zeta potentials observed at pH values smaller than IEP suggest the protonation of such functionalities owing to the great concentrations of H^+ ions.

The WP treatment of PPT-coated particles for durations up to 10 min not only significantly reduces the zeta potentials but also shifts the IEP to pH values less than 3.5. Such changes in electrokinetic properties follow the trends of $-SO_x(H)$ concentration observed from XPS (Figure 3) and TOF-SIMS (Figure 4) data. It can therefore be suggested that the introduced negatively charged moieties such as sulfonate (SO_3) and sulfate (SO_4) together with the deprotonation of strong acidic groups such as sulfonic acid ($SO_3H + H_2O \rightarrow SO_3^- + H_3O^+$) play a significant role in the modification of electrokinetic properties of silica particles. The plasma treatment of PPT-coated particles for 10 min results in lower zeta potentials in comparison with the treatment time of 2 min, as higher concentrations of negatively charged groups are likely to be obtained on the surface due to a longer treatment time. Water plasma treatment of particles for 60 min, however, results in an increase in overall zeta potential and IEP. Such behavior is once again in agreement with the surface chemistry results that suggested a lower concentration of sulfur-containing groups on the surface due to the pronounced influence of the ablation process. The electrokinetic analysis findings confirm that the combination of thiophene plasma polymerization and WP treatment produces highly negatively charged particles with significantly low IEPs.

3.4. Influence of Water Plasma Treatment Time and Initial Solution pH on Metal Removal Efficiency. Metal cations can adsorb onto any negatively charged surface via a simple electrostatic interaction.[16] The magnitude of negative zeta potential and the IEP of a surface are therefore crucial characteristics influencing the efficiency of cationic contaminant removal. As discussed in Section 3.3, WP treatment time of PPT-coated particles significantly improved these characteristics. The effectiveness of developed surfaces in heavy metal removal was investigated through adsorption of copper and zinc ions as model positively charged contaminants, while WP treatment time was varied. The initial solution pH is also one of the most important parameters governing the adsorption of metal ions through influencing the solution chemistry and ionization of surface functionalities.[13] At pH values lower than ~6, copper and zinc metal ions are in the predominant forms of Cu^{2+} and Zn^{2+}.[14,47−49] At higher pH values, hydrolysis of zinc and copper ions may form other complexes such as $Cu(OH)^+$ and $Zn(OH)^+$ together with precipitates of $Cu(OH)_2$ and $Zn(OH)_2$.[50,51] To avoid the interference of such a precipitation mechanism in the adsorption process, removal tests were conducted at pH values less than 6.

The influence of WP treatment time and initial pH of solution on the MRE of particles is shown in Figure 7. Clearly,

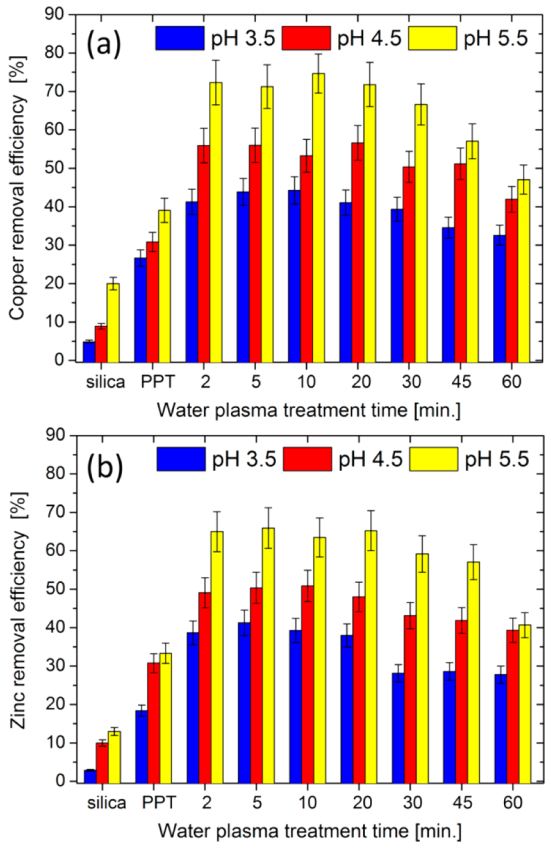

Figure 7. Influence of WP treatment time and initial pH of solution on the MRE of PPT-coated particles for (a) copper and (b) zinc. (C_i = 15 mg/L, removal time = 10 min, particle mass = 2 g/10 mL).

both untreated and WP-treated PPT-coated particles show significantly higher MRE values for all pH values in comparison to uncoated silica particles. Increasing the WP treatment time to 20 min significantly increases the MRE values for both copper and zinc ions. Further increasing the plasma treatment time, however, results in a noticeable decrease in MRE. The presence of high-density −SH functionalities on the surface of untreated PPT-coated particles, as observed from TOF-SIMS

DOI: 10.1021/am508637k
ACS Appl. Mater. Interfaces 2015, 7, 4265−4274

images (Figure 4), may explain the higher MREs obtained for PPT-coated particles compared to uncoated silica particles. The significant improvement in the adsorption behavior of WP-PPT-coated particles correlates with the variations of $-SO_x(H)$ group concentration (Figures 3 and 4) and surface zeta potential (Figure 6) as a function of plasma treatment time. As more $-SO_x(H)$ functionalities are generated onto silica particles at longer plasma treatment times, surfaces with lower zeta potentials are produced, thus also resulting in a greater driving force for metal cations to adsorb via electrostatic attraction. The presence of sulfonic acid groups (SO_3H) and reactive basic centers such as $-SH$ functionalities on the surface of modified particles (Figure 4) may also enhance the adsorption of metal cations through pH-dependent complexation and ion-exchange reactions.[52,53]

The decrease of MREs for treatment times of 30−60 min can be attributed to the ablation mechanism of sulfur-containing groups, as suggested by surface chemistry results. The reduction of MRE is however less significant compared to the reduction of sulfur atomic concentration observed in Figure 1. Such a discrepancy can be explained simply by the higher surface sensitivity of the adsorption process, which only sees the very topmost of a surface. A significant proportion of the WP-PPT film should therefore be ablated away before it affects the MRE.

From Figure 7, it can be observed that the MRE is smaller for lower pH values for all uncoated, untreated and WP-treated PPT-coated silica particles. The greatest adsorption of metal ions is achieved at pH = 5.5. For uncoated silica particles, for example, MREs of ∼20% and 13% are observed at pH = 5.5 for copper and zinc, respectively, whereas these values decrease to ∼3% and 5% at pH = 3.5. The low MREs of uncoated silica particles at pH = 3.5 is attributed to their relatively high IEP of pH ≈ 5 (Figure 6), resulting in an increase in the concentration of positively charged ($-Si-OH_2^+$) groups on the surface due to protonation. The positively charged groups therefore repel the cationic metal ions from the surface,[54] also significantly decreasing the MRE. The competition between metal ions and protons (H^+) becomes more significant at acidic conditions, which may also play a role in reducing the MRE.[20,50,51] In contrast to uncoated silica particles, the protonation of WP-PPT-coated particles occurs at significantly lower pH values (IEP < 3.5), as discussed in Section 3.3. Such low IEPs result in greater electrostatic attractions at lower pH values, which therefore increase the MRE. The adsorption capability of WP-PPT-coated particles at acidic conditions is of particular interest as many of the heavy metal adsorbents reported in the literature suffer from poor removal efficiencies at low pH values due to their relatively high IEPs.[50,51] According to the obtained results, the maximum MRE for both copper and zinc ions is achieved at a treatment time of 10 min, where the greatest concentration of $-SO_x(H)$ functionalities is generated on the surface. PPT-coated particles treated for 10 min were therefore applied for time and particle mass variable removal experiments.

3.5. Influence of Removal Time on Metal Removal Efficiency. Time-variable heavy metal removal was investigated to determine the removal kinetics and the time required for an optimum removal. These experiments were conducted using WP-PPT-coated particles treated for 10 min, while the optimum pH value of 5.5 was kept constant. As shown in Figure 8, the MREs sharply increase during the first 30 min, while reaching their maximum values after removal times of 60 min. By further increasing the removal time, MREs do not change significantly. The higher rate of adsorption at initial stages of interaction can be attributed to a greater difference between the concentration of metal ions in solution and those on the surface of WP-PPT-coated particles.[13] Higher numbers of free surface functionalities initially available on the particles may also provide easier accessibility of metal ions to unoccupied adsorption sites. The lower uptake rates of copper and zinc ions observed at longer removal times can be assigned to a decrease in the number of vacant adsorption sites as well as metal ion concentrations.[2,55] Nonporous WP-PPT-coated silica particles exhibit significantly faster adsorption kinetics in comparison to porous adsorbents such as zeolites[12] and fly ash pellets[56] as the diffusion of ions into a porous structure is not involved in the adsorption mechanism.

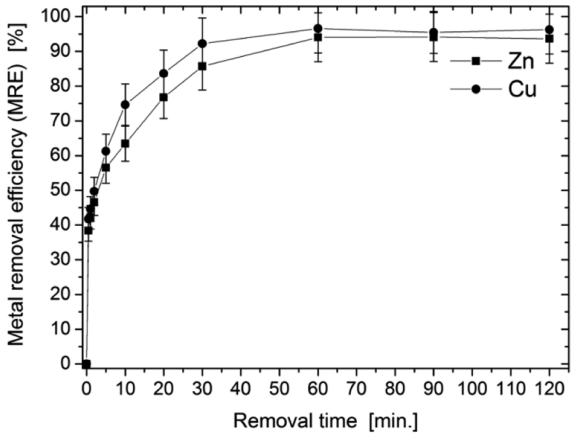

Figure 8. MRE for WP-PPT-coated particles as a function of removal time. (WP treatment time = 10 min, C_i = 15 mg/L, particle mass = 2 g/10 mL).

It is observed that slightly higher MREs are achieved for copper ions compared to zinc. Such a difference may be attributed to differences in electronegativity and the first hydrolysis equilibrium constants of copper and zinc ions.[57] For an ion exchange mechanism, heavy metals possessing a higher charge-to-mass ratio react more easily with a protonated site in comparison to less acidic metal ions.[58] Greater adsorption of copper compared to zinc has also been observed previously for other adsorbents.[12,57]

3.6. Influence of Adsorbent Dose on Metal Removal Efficiency. The influence of adsorbent dose on the heavy metal removal was investigated with particle masses of 0.25−5 g/10 mL at a constant pH of 5.5. To ensure the achievement of an equilibratory adsorption, a removal time of 60 min was kept unchanged for these experiments. As shown in Figure 9, MRE increases for both copper and zinc ions upon an initial increase of particle mass and reaches a maximum of more than 96.7% for an adsorbent dose of 3 g/10 mL. The lower MREs observed at smaller adsorbent doses indicate the lack of sufficient adsorption sites for the number of zinc and copper ions in solution. Increasing the adsorbent doses therefore increases the MRE due to additional adsorption sites. Increasing the mass of particles over 3 g/10 mL noticeably decreases the MRE, despite the addition to the total number of adsorption sites in solution. Such behavior can be explained by obscuration of adsorption sites. As more silica particles are added to a constant volume of solution, even with high degrees of agitation, the particle−particle interactions become more pronounced.[13] These interactions may physically block the available adsorption sites, thus also decreasing the MRE. A similar trend in changes

DOI: 10.1021/am508637k
ACS Appl. Mater. Interfaces 2015, 7, 4265−4274

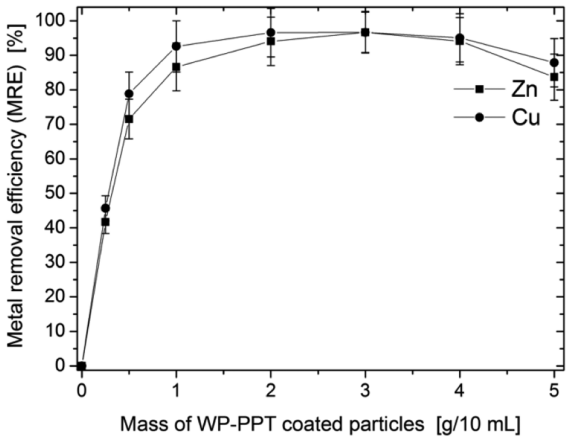

Figure 9. MRE for WP-PPT-coated particles as a function of particle mass. (WP treatment time = 10 min, C_i = 15 mg/L, removal time = 60 min.).

of MRE as a function of adsorbent dose has also been previously reported.[11,13] From Figure 9, it is observed that a slightly higher MRE is achieved for copper than zinc for most adsorbent doses. These data are in accordance with the results of removal time studies (Figure 8) and once again confirm the easier removal of copper compared to zinc.

The effectiveness of WP-PPT-coated particles in the removal of copper and zinc ions is compared with a number of other adsorbents listed in Table 1. Although a direct comparison of adsorbents is not practically possible due to different experimental conditions such as solution pH, plasma polymer functionalized particles are among the most efficient adsorbents. The maximum removal efficiency and maximum adsorption capacity of WP-PPT-coated particles are either comparable or higher than other adsorbents. Moreover, the waste-free and substrate-independent production process of WP-PPT-coated particles makes them attractive adsorbents for the removal of heavy metal ions. According to obtained results, it can be concluded that our introduced plasma-assisted method is effective for the development of efficient negatively charged adsorbents with excellent affinity for copper and zinc ions. Any other positively charged species could theoretically also be removed via WP-PPT-coated particles owing to the contaminant-independent electrostatic interaction.

4. CONCLUSIONS

The application of a new class of synthetic adsorbent materials for the removal of heavy metal ions was reported in this research. Sulfur-containing groups were initially deposited onto the surface of silica particles via thiophene plasma polymerization. Subsequent oxidative WP treatments of PPT-coated particles resulted in substantial formation of $-SO_x(H)$ groups as suggested by XPS, TOF-SIMS, and electrokinetic analyses data. It has been demonstrated that controlling the concentration of $-SO_x(H)$ functionalities on the surface tailors the zeta potential and IEPs of particles, thus also controlling the magnitude of heavy metal removal. WP-PPT-coated particles showed excellent affinity for both zinc and copper ions, removing more than 96.7% of metal ions in 60 min. Water plasma treatment of PPT-coated particles for shorter durations of 5−20 min showed greater removal efficiency in comparison to longer durations of 30−60 min, due to the influence of the ablation mechanism of sulfur-containing groups. Plasma polymerization of thiophene onto silica particles followed by WP treatment is a successful approach for the fabrication of efficient heavy metals adsorbents. This novel substrate-independent approach could be utilized to convert other inexpensive natural materials to high-value adsorbents.

AUTHOR INFORMATION

Corresponding Author

*Phone: +61 8 83023162. Fax: +61 8 83023380. E-mail: peter.majewski@unisa.edu.au.

Notes

The authors declare no competing financial interest.

ACKNOWLEDGMENTS

The authors gratefully acknowledge the financial support of Government of South Australia, through the Premier Science and Research Fund (PSRF) and the National Centre of Excellence in Desalination Australia (NCEDA). The authors acknowledge the facilities and scientific and technical assistance of the Australian Microscopy & Microanalysis Research Facility at the South Australian Regional Facility (SARF), University of South Australia, a facility that is funded by the University and by State and Federal Governments. We are thankful to Mr. Stuart McClure for conducting ESEM and to Dr. J. Denman for undertaking TOF-SIMS measurements.

Table 1. Maximum Adsorption Capacity, Maximum Removal Efficiency, and Optimum Removal Time for Plasma Polymer Functionalized Silica Particles and a Number of Other Copper and Zinc Adsorbents Reported in the Literature

adsorbent	adsorbate	maximum adsorption capacity [mg/g]	maximum removal efficiency [%]	optimum removal time	solution pH	ref
plasma polymer functionalized silica particles	Cu	25.0	>96.7	60 min	5.5	present work
	Zn	27.4	>96.7	60 min		
polyvinyl alcohol (PVA)/(EDTA) resin	Zn	38.6	~75	90 min	5	5
graphene oxide/Fe_3O_4 composites	Cu	18.3	~55	10 h	5.3	48
aminated electrospun polyacrylonitrile microfiber	Cu	~24	~60	12 h	4	2
aminated electrospun polyacrylonitrile nanofiber	Cu	~36	~90	12 h	4	2
bentonite	Zn	~20	~80	6 h	4	50
MnO_2-coated magnetic nanocomposites	Cu	not reported	~97	30 min	6.3	59
	Zn		~80	30 min		
fly ash	Zn	not reported	~98	3 h	6	55

DOI: 10.1021/am508637k
ACS Appl. Mater. Interfaces 2015, 7, 4265−4274

REFERENCES

(1) Shannon, M. A.; Bohn, P. W.; Elimelech, M.; Georgiadis, J. G.; Marinas, B. J.; Mayes, A. M. Science and Technology for Water Purification in the Coming Decades. *Nature* **2008**, *452*, 301−310.

(2) Kampalanonwat, P.; Supaphol, P. Preparation and Adsorption Behavior of Aminated Electrospun Polyacrylonitrile Nanofiber Mats for Heavy Metal Ion Removal. *ACS Appl. Mater. Interfaces* **2010**, *2*, 3619−3627.

(3) Fu, F. L.; Wang, Q. Removal of Heavy Metal Ions from Wastewaters: A Review. *J. Environ. Manage.* **2011**, *92*, 407−418.

(4) Shawabkeh, R.; Al-Harahsheh, A.; Al-Otoom, A. Copper and Zinc Sorption by Treated Oil Shale Ash. *Sep. Purif. Technol.* **2004**, *40*, 251−257.

(5) Zhang, Y.; Li, Y. F.; Yang, L. Q.; Ma, X. J.; Wang, L. Y.; Ye, Z. F. Characterization and Adsorption Mechanism of Zn^{2+} Removal by PVA/EDTA Resin in Polluted Water. *J. Hazard. Mater.* **2010**, *178*, 1046−1054.

(6) Jarup, L. Hazards of Heavy Metal Contamination. *Br. Med. Bull.* **2003**, *68*, 167−182.

(7) Fu, F. L.; Xie, L. P.; Tang, B.; Wang, Q.; Jiang, S. X. Application of a Novel Strategy-Advanced Fenton-chemical Precipitation to the Treatment of Strong Stability Chelated Heavy Metal Containing Wastewater. *Chem. Eng. J.* **2012**, *189*, 283−287.

(8) Zhang, Q.; Wang, N.; Zhao, L. B.; Xu, T. W.; Cheng, Y. Y. Polyamidoamine Dendronized Hollow Fiber Membranes in the Recovery of Heavy Metal Ions. *ACS Appl. Mater. Interfaces* **2013**, *5*, 1907−1912.

(9) Hunsom, M.; Pruksathorn, K.; Damronglerd, S.; Vergnes, H.; Duverneuil, P. Electrochemical Treatment of Heavy Metals (Cu^{2+}, Cr^{6+}, Ni^{2+}) from Industrial Effluent and Modeling of Copper Reduction. *Water Res.* **2005**, *39*, 610−616.

(10) Jiang, W.; Wang, W. F.; Pan, B. C.; Zhang, Q. X.; Zhang, W. M.; Lv, L. Facile Fabrication of Magnetic Chitosan Beads of Fast Kinetics and High Capacity for Copper Removal. *ACS Appl. Mater. Interfaces* **2014**, *6*, 3421−3426.

(11) Jarvis, K. L.; Majewski, P. Plasma polymerized allylamine coated quartz particles for humic acid removal. *J. Colloid Interface Sci.* **2012**, *380*, 150−158.

(12) Erdem, E.; Karapinar, N.; Donat, R. The Removal of Heavy Metal Cations by Natural Zeolites. *J. Colloid Interface Sci.* **2004**, *280*, 309−314.

(13) Sen, T. K.; Gomez, D. Adsorption of Zinc (Zn^{2+}) from Aqueous Solution on Natural Bentonite. *Desalination* **2011**, *267*, 286−294.

(14) Pehlivan, E.; Cetin, S.; Yanik, B. H. Equilibrium Studies for the Sorption of Zinc and Copper from Aqueous Solutions Using Sugar Beet Pulp and Fly Ash. *J. Hazard. Mater.* **2006**, *135*, 193−199.

(15) Eloussaief, M.; Jarraya, I.; Benzina, M. Adsorption of Copper Ions on Two Clays from Tunisia: pH and Temperature Effects. *Appl. Clay Sci.* **2009**, *46*, 409−413.

(16) Majewski, P. Interaction of Functionalised Surfaces on Silica with Dissolved Metal Cations in Aqueous Solutions. *Int. J. Mater. Res.* **2006**, *97*, 784−788.

(17) Xin, X.; Wei, Q.; Yang, J.; Yan, L.; Feng, R.; Chen, G.; Du, B.; Li, H. Highly Efficient Removal of Heavy Metal Ions by Amine-functionalized Mesoporous Fe3O4 Nanoparticles. *Chem. Eng. J.* **2012**, *184*, 132−140.

(18) Yantasee, W.; Rutledge, R. D.; Chouyyok, W.; Sukwarotwat, V.; Orr, G.; Warner, C. L.; Warner, M. G.; Fryxell, G. E.; Wiacek, R. J.; Timchalk, C.; Addleman, R. S. Functionalized Nanoporous Silica for the Removal of Heavy Metals from Biological Systems: Adsorption and Application. *ACS Appl. Mater. Interfaces* **2010**, *2*, 2749−2758.

(19) Qu, Q. S.; Gu, Q.; Gu, Z. L.; Shen, Y. Q.; Wang, C. Y.; Hu, X. Y. Efficient Removal of Heavy Metal from Aqueous Solution by Sulfonic Acid Functionalized Nonporous Silica Microspheres. *Colloids Surf., A* **2012**, *415*, 41−46.

(20) Elkady, M. F.; Abu-Saied, M. A.; Rahman, A. M. A.; Soliman, E. A.; Elzatahry, A. A.; Yossef, M. E.; Eldin, M. S. M. Nano-sulphonated Poly (Glycidyl Methacrylate) Cations Exchanger for Cadmium Ions Removal: Effects of Operating Parameters. *Desalination* **2011**, *279*, 152−162.

(21) Miller, A.; Wildeman, T.; Figueroa, L. Zinc and Nickel Removal in Limestone Based Treatment of Acid Mine Drainage: The Relative Role of Adsorption and Co-precipitation. *Appl. Geochem.* **2013**, *37*, 57−63.

(22) Akhavan, B.; Jarvis, K.; Majewski, P. Evolution of hydrophobicity in plasma polymerised 1,7-octadiene films. *Plasma Processes Polym.* **2013**, *10*, 1018−1029.

(23) Inagaki, N. *Plasma Surface Modification and Plasma Polymerization;* Technomic Pub. Co: Lancaster, PA, 1996.

(24) Michl, T. D.; Coad, B. R.; Hüsler, A.; Vasilev, K.; Griesser, H. J. Laboratory scale systems for the plasma treatment and coating of particles. *Plasma Processes Polym.* **2014**, DOI: 10.1002/ppap.201400141.

(25) Kim, J. W.; Choi, H. S. Surface crosslinking of high-density polyethylene beads in a modified plasma reactor. *J. Appl. Polym. Sci.* **2002**, *83*, 2921−2929.

(26) Murata, Y.; Aradachi, T. Change in charging characteristics of polymer powder by plasma treatment. *J. Electrost.* **2001**, *51*, 97−104.

(27) Shahravan, A.; Desai, T.; Matsoukas, T. Controlled manipulation of wetting characteristics of nanoparticles with dry-based plasma polymerization method. *Appl. Phys. Lett.* **2012**, *101*, 1−4.

(28) Akhavan, B.; Jarvis, K.; Majewski, P. Hydrophobic plasma polymer coated silica particles for petroleum hydrocarbon removal. *ACS Appl. Mater. Interfaces* **2013**, *5*, 8563−71.

(29) Akhavan, B.; Jarvis, K.; Majewski, P. Tuning the hydrophobicity of plasma polymer coated silica particles. *Powder Technol.* **2013**, *249*, 403−411.

(30) Jarvis, K. L.; Majewski, P. Influence of Film Stability and Aging of Plasma Polymerized Allylamine Coated Quartz Particles on Humic Acid Removal. *ACS Appl. Mater. Interfaces* **2013**, *5*, 7315−7322.

(31) Siow, K. S.; Britcher, L.; Kumar, S.; Griesser, H. J. Sulfonated surfaces by sulfur dioxide plasma surface treatment of plasma polymer films. *Plasma Processes Polym.* **2009**, *6*, 583−592.

(32) Inagaki, N.; Tasaka, S.; Miyazaki, H. Sulfonic Acid Group-containing Thin Films Prepared by Plasma Polymerization. *J. Appl. Polym. Sci.* **1989**, *38*, 1829−1838.

(33) Inagaki, N.; Tasaka, S.; Chengfei, Z. Preparation of Thin Films Containing Sulfonic Acid and Carboxylic Acid Groups by Plasma Polymerization of Perfluorobenzene/Sulfur Dioxide and Perfluorobenzene/Carbon Dioxide Mixtures. *Polym. Bull.* **1991**, *26*, 187−191.

(34) Akhavan, B.; Jarvis, K.; Majewski, P. Development of oxidized sulfur polymer films through a combination of plasma polymerization and oxidative plasma treatment. *Langmuir* **2014**, *30*, 1444−1454.

(35) Akhavan, B.; Jarvis, K.; Majewski, P. Plasma polymerization of sulfur-rich and water-stable coatings on silica particles *Surf. Coat. Technol.* DOI: 10.1016/j.surfcoat.2015.01.017.

(36) Silverstein, M. S.; Visoly-Fisher, I. Plasma Polymerized Thiophene: Molecular Structure and Electrical Properties. *Polymer* **2002**, *43*, 11−20.

(37) Hussain, S.; Amade, R.; Jover, E.; Bertran, E. Functionalization of Carbon Nanotubes by Water Plasma. *Nanotechnology* **2012**, *23*, 1−8.

(38) Mahdjoub, H.; Roualdes, S.; Sistat, P.; Pradeilles, N.; Durand, J.; Pourcelly, G. Plasma-Polymerised Proton Conductive Membranes for a Miniaturised PEMFC. *Fuel Cells* **2005**, *5*, 277−286.

(39) Tompkins, B. D.; Dennison, J. M.; Fisher, E. R. H2O Plasma Modification of Track-etched Polymer Membranes for Increased Wettability and Improved Performance. *J. Membr. Sci.* **2013**, *428*, 576−588.

(40) Crispin, X.; Marciniak, S.; Osikowicz, W.; Zotti, G.; Van der Gon, A. W. D.; Louwet, F.; Fahlman, M.; Groenendaal, L.; De Schryver, F.; Salaneck, W. R. Conductivity, morphology, interfacial chemistry, and stability of poly(3,4-ethylene dioxythiophene)-poly-(styrene sulfonate): A photoelectron spectroscopy study. *J. Polym. Sci., Part B: Polym. Phys.* **2003**, *41*, 2561−2583.

(41) Hollander, A.; Kropke, S. Polymer surface treatment with SO_2-containing plasmas. *Plasma Processes Polym.* **2010**, *7*, 390−402.

DOI: 10.1021/am508637k
ACS Appl. Mater. Interfaces 2015, 7, 4265−4274

(42) Vickerman, J. C.; Briggs, D. *TOF-SIMS: Surface Analysis by Mass Spectrometry;* IM Publications and Surface Spectra: Chichester, Manchester, U.K., 2001.
(43) Shin, Y. C.; Lee, D.; Lee, K.; Ahn, K. H.; Kim, B. Surface Properties of Silica Nanoparticles Modified with Polymers for Polymer Nanocomposite Applications. *J. Ind. Eng. Chem.* **2008**, *14*, 515−519.
(44) Majewski, P. J.; Fuchs, T. M. Variation of the Surface Charge of Silica Particles by Functionalised Self-assembled Monolayers. *Adv. Powder Technol.* **2007**, *18*, 303−310.
(45) Jimbo, T.; Higa, M.; Minoura, N.; Tanioka, A. Surface Characterization of Poly(Acrylonitrile) Membranes Graft-polymerized with Ionic Monomers as Revealed by Zeta Potential Measurement. *Macromolecules* **1998**, *31*, 1277−1284.
(46) Behrens, S. H.; Grier, D. G. The Charge of Glass and Silica Surfaces. *J. Chem. Phys.* **2001**, *115*, 6716−6721.
(47) Seco, A.; Gabaldon, C.; Marzal, P.; Aucejo, A. Effect of pH, Cation Concentration and Sorbent Concentration on Cadmium and Copper Removal by a Granular Activated Carbon. *J. Chem. Technol. Biotechnol.* **1999**, *74*, 911−918.
(48) Li, J.; Zhang, S. W.; Chen, C. L.; Zhao, G. X.; Yang, X.; Li, J. X.; Wang, X. K. Removal of Cu(II) and Fulvic Acid by Graphene Oxide Nanosheets Decorated with Fe3O4 Nanoparticles. *ACS Appl. Mater. Interfaces* **2012**, *4*, 4991−5000.
(49) Charles, F. B.; Mesmer, R. E. *The Hydrolysis of Cations;* Wiley: New York, 1976.
(50) Kaya, A.; Oren, A. H. Adsorption of Zinc from Aqueous Solutions to Bentonite. *J. Hazard. Mater.* **2005**, *125*, 183−189.
(51) Chu, K. H.; Hashim, M. A. Adsorption of Copper(II) and EDTA-chelated Copper(II) onto Granular Activated Carbons. *J. Chem. Technol. Biotechnol.* **2000**, *75*, 1054−1060.
(52) Guerra, D. L.; Airoldi, C. Anchored Thiol Smectite Clay - Kinetic and Thermodynamic Studies of Divalent Copper and Cobalt Adsorption. *J. Solid State Chem.* **2008**, *181*, 2507−2515.
(53) Machado, R. S. A.; da Fonseca, M. G.; Arakaki, L. N. H.; Espinola, J. G. P.; Oliveira, S. F. Silica Gel Containing Sulfur, Nitrogen and Oxygen as Adsorbent Centers on Surface for Removing Copper from Aqueous/Ethanolic Solutions. *Talanta* **2004**, *63*, 317−322.
(54) Kubilay, S.; Gurkan, R.; Savran, A.; Sahan, T. Removal of Cu(II), Zn(II) and Co(II) Ions from Aqueous Solutions by Adsorption onto Natural Bentonite. *Adsorption* **2007**, *13*, 41−51.
(55) Mishra, P. C.; Patel, R. K. Removal of Lead and Zinc Ions from Water by Low Cost Adsorbents. *J. Hazard. Mater.* **2009**, *168*, 319−325.
(56) Papandreou, A. D.; Stournaras, C. J.; Panias, D.; Paspaliaris, I. Adsorption of Pb(II), Zn(II) and Cr(III) on Coal Fly Ash Porous Pellets. *Miner. Eng.* **2011**, *24*, 1495−1501.
(57) Veglio, F.; Esposito, A.; Reverberi, A. P. Copper Adsorption on Calcium Alginate Beads: Equilibrium pH-related Models. *Hydrometallurgy* **2002**, *65*, 43−57.
(58) Pagnanelli, F.; Esposito, A.; Veglio, F. Multi-metallic Modelling for Biosorption of Binary Systems. *Water Res.* **2002**, *36*, 4095−4105.
(59) Kim, E. J.; Lee, C. S.; Chang, Y. Y.; Chang, Y. S. Hierarchically Structured Manganese Oxide-coated Magnetic Nanocomposites for the Efficient Removal of Heavy Metal Ions from Aqueous Systems. *ACS Appl. Mater. Interfaces* **2013**, *5*, 9628−9634.

DOI: 10.1021/am508637k
ACS Appl. Mater. Interfaces 2015, 7, 4265−4274